Appl. Phys. B 86, 425–429 (2007)
DOI: 10.1007/s00340-006-2557-7

Applied Physics B
Lasers and Optics

L. FU✉
H. SCHWEIZER
H. GUO
N. LIU
H. GIESSEN

Analysis of metamaterials using transmission line models

4th Physics Institute, University of Stuttgart, Pfaffenwaldring 57, 70550 Stuttgart, Germany

Received: 11 August 2006
Published online: 20 January 2007 •

ABSTRACT We use simple transmission line models with lumped elements of inductance and capacitance to interpret optical transmission and reflection spectra of cut wires and cut-wire pairs in the near infrared region. The numerical values of the elements are obtained by fitting experimental or numerical simulated reflectance and transmittance spectra. The scattering parameters and the retrieved effective material parameters calculated from the transmission line models show good agreements with those obtained from experiments or numerical simulations. This indicates that transmission line theory is a powerful tool for designing and analyzing metamaterials at optical frequencies.

PACS 41.20.Jb; 78.67.-n; 78.66.Sg

1 Introduction

Metamaterials are artificial metallic structures designed to exhibit novel electromagnetic properties, which are normally not found in nature. The size of the structures is typically smaller than the free space wavelength of incoming light. Metamaterials with simultaneously negative permittivity and permeability, which are known as left-handed materials (LHMs) or negative index materials (NIMs), have promising application potential, such as designing perfect lenses to surpass the diffraction limit [1, 2]. After the first demonstration of negative refraction at GHz frequencies [3], this topic has since become very attractive at optical frequencies [4, 5].

Transmission line (TL) theory is of significant importance in microwave network analysis. It was extended to treat scattering problems of electromagnetic waves on discontinuous metallic structures [6]. Recently, transmission line models (TLMs) were extensively employed to analyze metamaterials in the GHz regime [8–11]. From this theory it is known that the magnetic permeability μ in a homogeneous material is determined by series per unit length impedance, i.e., $Z' = j\omega\mu$, while the electric permittivity ε is determined by shunt per unit length admittance, i.e., $Y' = j\omega\varepsilon$ [8, 9]. Accordingly, a TLM was suggested for LHMs and lumped elements were implemented to obtain an 1- or 2-D broadband NIM in the microwave frequency region [8, 11].

From the viewpoint of inductive and capacitive elements, the behavior of metallic structures at optical frequencies is not as clear as at microwave frequencies [6]. Recently, a concept of circuit nanoelements in the optical domain was suggested [7]. Nevertheless, if metamaterials at optical frequencies can also be represented by simple equivalent circuits, more physical insight into the behavior of such materials and the correlation of ε and μ to shunt or series circuit elements can be gained.

In this report, we first review the transmittance spectra of five simple two-port two-element TLMs. Then we approach the analysis of cut wires and cut-wire pairs in the near infrared region using TLMs. The procedure is as follows: *S*-parameters (namely, scattering parameters of a TL network. S_{ii} is the reflection coefficient seen looking into port i and the S_{ij} is the transmission coefficient from port j to port i [12]) are first calculated according to our suggested TLMs for the metamaterials. The values of L and C are chosen appropriately by fitting the corresponding experimental or numerical simulation results. If the scattering parameters of the metamaterial can be reproduced, then we conclude that the TLM represents the metamaterial reasonably well.

2 Spectra of typical TL equivalent circuits

The study in this report is based on one-dimensional TLMs for a single polarization. In TL theory, both elements which interact with an EM wave and the path along which the wave propagates can be described using ABCD matrices. The total matrix is just the product of the matrices of the propagating wave. A relationship between the ABCD matrix and the scattering parameters exists [12]. Using this relationship, transmittance and reflectance spectra can be calculated, and effective material parameters can be retrieved [13, 14]. In the calculation, the lumped elements are assumed to be dimensionless and the length of the TL is given by ΔZ. It accounts for the wave propagation length in vacuum, which is comparable to the light path used in our numerical simulations. In all of the TLMs, the input electromagnetic wave propagates from left to right. This corresponds to the incident light coming from above into the substrate in the numerical setup.

✉ Fax: +49-711-68565097, E-mail: L.Fu@physik.uni-stuttgart.de

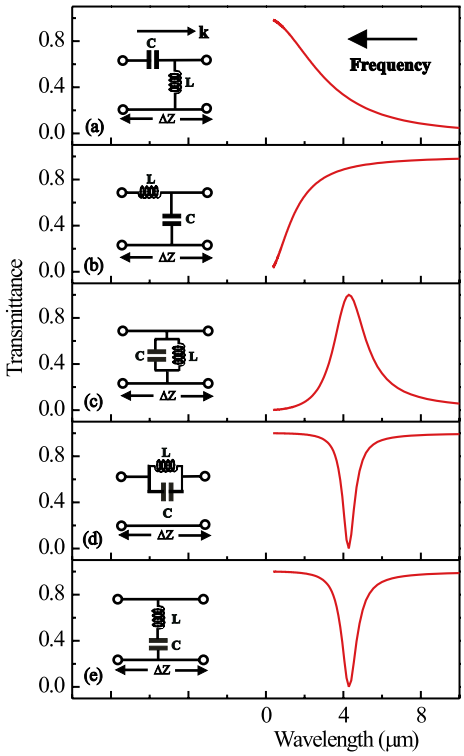

FIGURE 1 Five two-port two-element TLMs and their corresponding transmittance spectra. (**a**) A pure left-handed TLM shows a high pass behavior in frequency. (**b**) A pure right-handed TLM shows a low pass behavior in frequency. (**c**) A TLM with parallel combination of L and C in shunt results in a band pass behavior. (**d**) A TLM with parallel combination of L and C in series results in a band rejection behavior. (**e**) A TLM with series combination of L and C in shunt also results in a band rejection behavior

In Fig. 1, five common two-port two-elements TLMs and their corresponding transmittance spectra are shown. In general, a resistance must be included to account for losses, but is omitted here for simplicity.

Each model circuit has an inductance (L) and a capacitance (C) combined differently in the TL. Some of them display a resonant behavior. Circuit (a) consists of a combination of a series C and a shunt L in the TL. It yields high pass characteristics in the frequency domain. This circuit supports backwards travelling waves and can therefore represent LHMs [8]. Circuit (b) uses a combination of a series L and a shunt C in the TL, which results in a low pass band of the frequency. This is the classic lumped model for coaxial cables and other similar waveguides. Circuit (c) is composed of a parallel combination of L and C in shunt in the TL. It provides a band pass behavior and was used to represent inductive grids at far infrared frequencies [15]. Circuit (d) is composed of a parallel combination of L and C in series in the TL. It shows a band rejection behavior and was used to interpret split ring resonators at GHz frequencies [10]. In fact, it can describe any magnetic resonances as we will show in [16], even at optical frequencies. Circuit (e) is composed of a series combination of L and C in shunt in the TL. It shows also a band rejection behavior. At far infrared frequencies, it was used to represent capacitive plates (or equivalently, cut wires) [15]. Generally, the situation may be more complex, especially considering the less than clear nature of L and C at very high frequencies.

3 TLM for one-layer 2D gold cut wires

To consider the application of the TL theory at optical frequencies, we start with a simple structure, namely a single layer of 2-dimensional (2D) periodic gold cut wires on a glass substrate. Figure 2a shows a pictorial of a cut-wire setup with two unit cells and a TLM schematic. Plots of calculated and simulated spectra are shown in Fig. 2b and c. The Au cut wires have a thickness of 20 nm, a length of 500 nm with 1050 nm period, and a width of 150 nm with 500 nm period. The glass substrate has a refractive index of 1.5. Incident light comes from above with an orientation of the electric field vector E along the length of the wires.

A commercial electromagnetic simulator was used to study the structure [17]. To compare with the results from the TLMs, the sample system considered includes the space above the structure (in vacuum), the space beneath the structure (in the substrate), and the physical thickness of the structure. By retrieval of the effective material parameters [14],

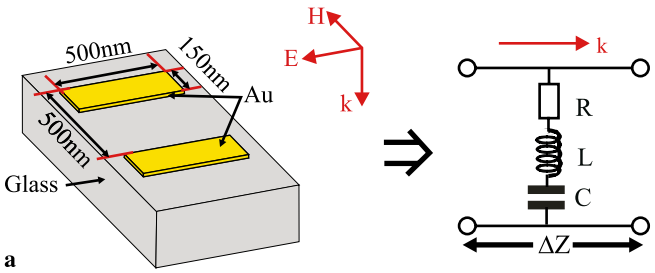

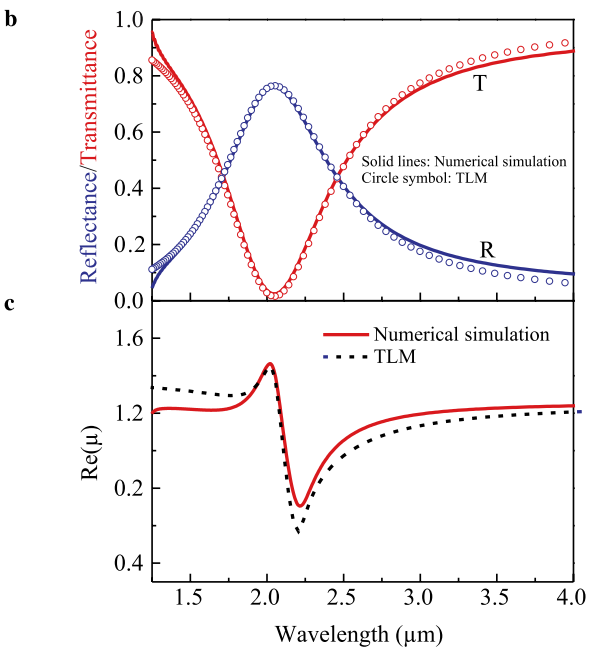

FIGURE 2 (**a**) Pictorial of one layer cut-wire setup with two unit cells and its corresponding TLM. (**b**) Comparison of R/T-curves from the numerical simulation (*solid lines*) and fit curves from the TLM (*open circles*). (**c**) Comparison of the real part of μ retrieved from numerical results with that retrieved from the TLM

Element	L ($\times 10^{-13}$ H)	C ($\times 10^{-19}$ F)	R (Ω)
Value	5.63	20.5	33

TABLE 1 Values of the circuit elements in the TLM shown in Fig. 2a to fit the simulated spectra in Fig. 2b

the whole system is assumed to be homogenous. Including the light path in vacuum and in the substrate does not change the form of the reflectance/transmittance (R/T) spectra nor the resonant behavior of the effective materials parameters. Assuming that elements located perpendicular to the wave propagation are shunt elements, a series combination of L and C in shunt in the TL (circuit (e) in Fig. 1) is chosen as the TLM for the cut wires, as was used in the far infrared region [15]. A resistance R for loss is also added for better adapting of the simulated curves.

In Fig. 2b, R/T-spectra from the numerical simulation are compared with the fit curves from the TLM. Fitting the TLM equations to the simulation curves gives the appropriate values of L, C, and R, which are listed in Table 1. The fitted curve shapes agree well with the simulated results. In Fig. 2c, the real part of the retrieved μ is compared with the one retrieved from the numerical results. Both curves show an identical resonance behavior, which is typical for cut wires [16]. The small offset at higher frequency is induced by the higher order mode in the numerical results, which is not considered in the TLM. Evidently, the behavior of such a system is well modelled by such a simple circuit.

4 TLM for 2D cut-wire pairs

To employ the TL theory to actual experimental results [5], we further study 2D periodic cut-wire pairs with a similar structure size as that single layer cut wires. The cut-wire pairs are separated by a spacer layer 80 nm MgF_2. Structure details can be found in [5]. Incident light propagates again from above and the electric field is along the length of the wires.

The TLM for the cut-wire pairs used here is an extension of the model for single layer cut wires, which is illustrated in Fig. 2a. Each layer is modelled by the shunt elements, and the length d models the spacer layer. The interactions between the two sites along the transmission line is neglected here and is discussed in Sect. 5.

Using this model the experimental results are fitted. The plots in Fig. 4a show the measured transmittance and reflectance versus wavelength for the cut-wire pairs with lengths of 500, 400, and 300 nm [5]. The plots in Fig. 4b are the fit curves for the TLM shown in Fig. 3. For these plots, the TL equations of the model were fitted to the experimental data for appropriate values of L, C, and R, which are listed in Table 2. Different lengths of cut-wire pairs have different resonant frequencies, and therefore different values of L and C. In addition, the top layer in the experimental cut-wire pairs is responsible for the short-wavelength resonance (λ_1), and the bottom layer is responsible for the long-wavelength resonance (λ_2). The agreement in spectral behavior is an indication that the TLM does represent the cut-wire pair structure.

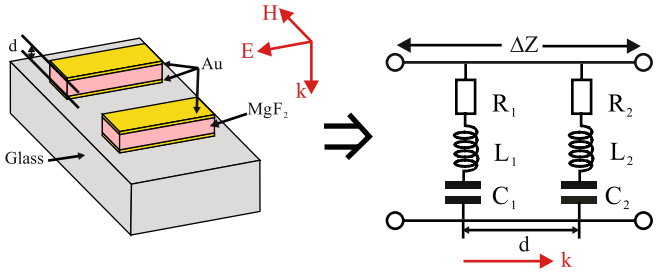

FIGURE 3 Setup pictorial of cut-wire pairs and a corresponding circuit model. The shunt elements of R_1, L_1, and C_1 model the resonance of the top layer cut wires and R_2, L_2, and C_2 model the resonance of the bottom layer cut wires; d models the space layer

Resonance (wire length, nm)	L ($\times 10^{-13}$ H)	C ($\times 10^{-19}$ F)	R (Ω)
λ_1 (500)	6.3	9.5	120
λ_2 (500)	22.3	4.8	165
λ_1 (400)	10.3	4.3	210
λ_2 (400)	18.6	4.0	180
λ_1 (300)	14.9	1.8	380
λ_2 (300)	14.5	3.1	210

TABLE 2 Values of circuit elements in the TLM shown in Fig. 3 to get the fitted curves shown in Fig. 4b

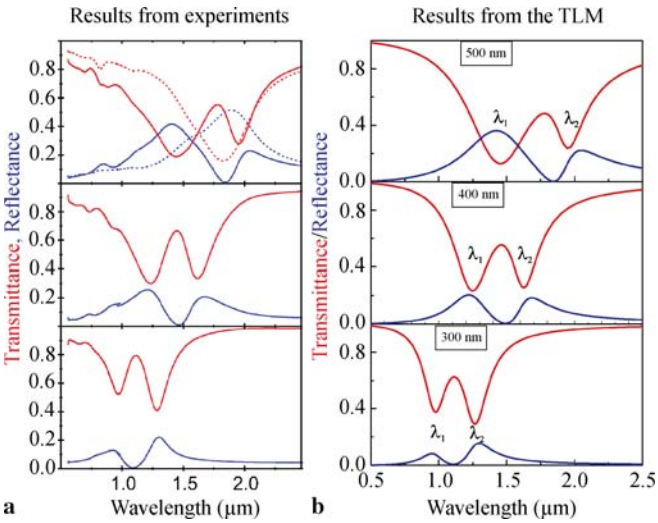

FIGURE 4 (**a**) Experimental R/T-spectra for 500 nm, 400 nm, and 300 nm long cut-wire pairs [5]. The *dotted lines* are for single layer cut wires. (**b**) Fitted R/T-spectra of the corresponding cut-wire pairs using the TLM shown in Fig. 3

5 Coupling between the cut-wire pairs

If each cut wire in the cut-wire pairs can be taken as a harmonic oscillator, the coupling between the two is strongest when they are identical. Such a coupling occurs along the wave propagation and induces a magnetic resonance in the given polarization, which can be represented by circuit (d) in Fig. 1. However, with the experimental structure fabricated on a glass substrate, the coupling between the wire pair is weakened due to two effects. The first is induced by the lift-off procedure. It causes the size of the top wire to be smaller than that of the bottom wire [5]. This weakening effect can be observed through the retrieved real part of μ. Compared to the value of the real part of μ for the magnetic resonance

mode with size-identical cut-wire pairs, it is smaller with size-asymmetric cut-wire pairs. The second effect is induced by the presence of the substrate. This results in an environment with higher effective refractive index for the bottom wire. Both effects shift the resonance frequency of the bottom wire to red. Therefore, for the actual structure as fabricated in [5], the longitudinal coupling between the cut-wire pairs is rather weak. This can also be clarified using TLMs.

We use two TLMs to represent the two cases: strong coupling (circuit I) and weak coupling (circuit II), as shown in Fig. 5. The values of L, C, and R for obtaining the spectra in Fig. 5a–d are listed in Table 3. In circuit I, the combination of L_1, C_1, and R_1 models the symmetric resonance mode (cut-wire mode), and the combination of L_c, C_c, and R_c models the antisymmetric resonance mode (coupling mode). As we can see from Fig. 1, both the cut-wire mode (circuit (e) in Fig. 1) and the coupling mode (or magnetic resonance mode, circuit (d) in Fig. 1) have a band rejection behavior. However, when they are combined together, the form of the resultant R/T-spectra is different when compared to that from the TLM shown in Fig. 3, which is combined by two cut-wire modes. Introducing resistors R_1 and R_c, the transmittance spectrum can be adapted to a similar form as the experimental one, as is shown in Fig. 5b. However, the reflectance on the long wavelength side is strongly suppressed, regardless of the variation

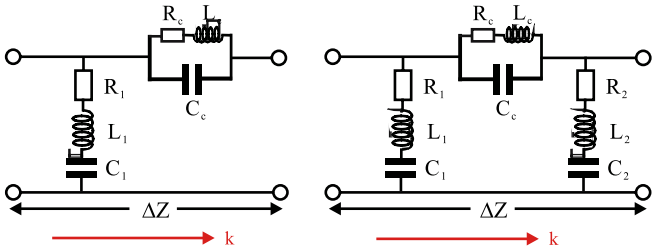

(I) Strong coupling; (II) Weak coupling.

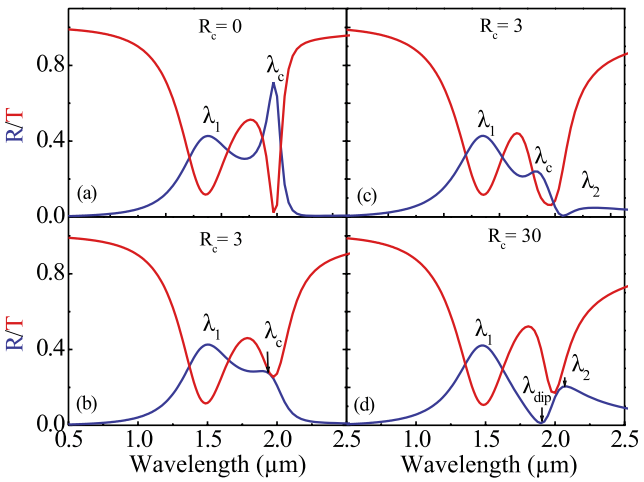

FIGURE 5 Circuit I: TLM for strongly coupled cut-wire pairs. Circuit II: TLM for weakly coupled cut-wire pairs. Resonance wavelength λ_c corresponds to the resonance induced by the coupling mode and λ_i corresponds to the cut-wire mode of the top layer (with $i = 1$) or the bottom layer (with $i = 2$). The plots show calculated R/T-spectra in order to fit experimental results of 500 nm cut-wire pairs, using (**a**) circuit I with $R_c = 0\,\Omega$, (**b**) circuit I with $R_c = 3\,\Omega$, (**c**) circuit II with $R_c = 3\,\Omega$, (**d**) circuit II with $R_c = 30\,\Omega$

Resonance	L ($\times 10^{-13}$ H)	C ($\times 10^{-19}$ F)	R (Ω)
λ_1	7.3	8.5	100
λ_c	0.37	277	varies
λ_2	30	3.7	155

TABLE 3 Values of the circuit elements in the TLM shown in Fig. 5 (I, II) to fit the simulated spectra in Fig. 5a–d

of L, C, and R. Additionally the dip in the reflectance spectra does not reach zero.

Considering the coupling between the cut-wire pairs and also assuming that there are still separate resonance modes for the top and bottom layer, respectively, a TLM can be constructed as shown in circuit II in Fig. 5. It is assumed that the coupling mode oscillates between the resonance frequencies of the two cut-wire modes. To fit the experimental R/T-spectra, we found that R_c has to be increased substantially until the spectra shown in (d) can be obtained. However, with this high value of R_c for losses, the coupling effect is already very weak and can be neglected.

In the numerical simulation for 500 nm cut-wire pairs on glass, field distributions away from the reflectance peak λ_2 at the long wavelength side shows that there exists only the oscillation of the bottom cut wire. This indicates further that the coupling occurs only in a narrow bandwidth and the reflectance amplitude at the long wavelength side is induced mainly by the resonance mode of the bottom cut wires.

6 Conclusion

We have studied cut wires and cut-wire pairs using transmission line models. The S-parameters calculated from the suggested TLMs show good agreement with simulation and experimental results. We also show that when the cut-wire pairs are located on a glass substrate with different size of the top and bottom cut wires, they behave mainly as two separate cut wires, and the coupling between the pairs can be neglected. The results of the TLMs in comparison with experiment or numerical simulations indicate that TL theory is a powerful analysis tool for metamaterials at optical frequencies. In fact, one can construct a TLM for any metamaterial based on its known measured or simulated S-parameters. In this sense, a TL-model describes a real material, but should not be considered as a material in its own right. Limitations of this description include a lack of angle and polarization dependence of the incident light. In the model, this could manifest itself in a change of L and C or a different circuit geometry. The number of lumped elements in a TLM may be not unique. However, while keeping the main character of the curves, the circuit with minimum number of elements is unique [16].

ACKNOWLEDGEMENTS We would like to thank DFG (SPP1113, FOR557 and 730), BMBF (13N8340 and 13N9155) and MWFK Baden-Württemberg (contract number: 24-753 23-15-17/1) for support, and T.P. Meyrath for discussions.

REFERENCES

1 V.G. Veselago, Sov. Phys. Uspekhi **10**, 509 (1968)
2 J.B. Pendry, Phys. Rev. Lett. **85**, 3966 (2000)
3 R.A. Shelby, D.R. Smith, S. Schultz, Science **292**, 77 (2001)

4 C. Enkrich, M. Wegener, S. Linden, S. Burger, L. Zschiedrich, F. Schmidt, J.F. Zhou, T. Koschny, C.M. Soukoulis, Phys. Rev. Lett. **95**, 203 901 (2005)
5 G. Dolling, C. Enkrich, M. Wegener, J. Zhou, C.M. Soukoulis, S. Linden, Opt. Lett. **30**, 3198 (2005)
6 N. Marcuvitz, J. Schwinger, J. Appl. Phys. **22**, 806 (1951)
7 N. Engheta, A. Salandrino, A. Alú, Phys. Rev. Lett. **95**, 095 504 (2005)
8 G.V. Eleftheriades, A.K. Iyer, P.C. Kramer, IEEE Trans. Microw. Theory Technol. **50**, 2702 (2002)
9 A. Lai, C. Caloz, T. Itoh, IEEE Microw. Mag. **Sept.**, 34 (2004)
10 G.V. Eleftheriades, O. Siddiqui, A.K. Iyer, IEEE Microw. Wireless Comp. Lett. **13**, 51 (2003)
11 C. Caloz, T. Itoh, IEEE Trans. Antennas Propag. **52**, 1159 (2004)
12 D.M. Pozar, *Microwave Engineering* (Wiley, New York, 2005), 3rd Edn., p. 187
13 A.M. Nicolson, G.F. Ross, IEEE Trans. Instrum. Meas. **19**, 377 (1970)
14 D.R. Smith, S. Schultz, Phys. Rev. B **65**, 195 104 (2002)
15 R. Ulrich, Infrared Phys. **7**, 37 (1967)
16 L. Fu, H. Schweizer, H. Guo, N. Liu, H. Giessen, to be published
17 CST Microwave Studio, Darmstadt, Germany